AP1B sorts basolateral proteins in recycling and biosynthetic routes of MDCK cells

Diego Gravotta*, Ami Deora*, Emilie Perret*, Claudia Oyanadel†‡, Andrea Soza†‡, Ryan Schreiner*, Alfonso Gonzalez†‡, and Enrique Rodriguez-Boulan*§

*Margaret Dyson Vision Research Institute, Weill Medical College of Cornell University, 1300 York Avenue, New York, NY 10021; †Departamento de Inmunología Clínica y Reumatología, Facultad de Medicina, and Centro de Regulación Celular y Patología, Facultad de Ciencias Biológicas, Pontificia Universidad Católica de Chile, 6510260 Santiago, Chile; and ‡Millennium Institute for Fundamental and Applied Biology, 7780344 Santiago, Chile

Communicated by David D. Sabatini, New York University School of Medicine, New York, NY, December 3, 2006 (received for review February 3, 2006)

The epithelial-specific adaptor AP1B sorts basolateral proteins, but the trafficking routes where it performs its sorting role remain controversial. Here, we used an RNAi approach to knock down the medium subunit of AP1B (μ1B) in the prototype epithelial cell line Madin–Darby canine kidney (MDCK). μ1B-knocked down MDCK cells displayed loss of polarity of several endogenous and exogenous basolateral markers transduced via adenovirus vectors, but exhibited normal polarity of apical markers. We chose two well characterized basolateral protein markers, the transferrin receptor (TfR) and the vesicular stomatitis virus G protein, to study the sorting role of AP1B. A surface-capture assay introduced here showed that μ1B-knocked down MDCK cells plated on filters at confluency and cultured for 4.5 d, sorted TfR correctly in the biosynthetic route but incorrectly in the recycling route. In contrast, these same cells missorted vesicular stomatitis virus G apically in the biosynthetic route. Strikingly, recently confluent MDCK cells (1–3 d) displayed AP1B-dependence in the biosynthetic route of TfR, which decreased with additional days in culture. Sucrose density gradient analysis detected AP1B predominantly in TfR-rich endosomal fractions in MDCK cells confluent for 1 and 4 d. Our results are consistent with the following model: AP1B sorts basolateral proteins in both biosynthetic and recycling routes of MDCK cells, as a result of its predominant functional localization in recycling endosomes, which constitute a post-Golgi station in the biosynthetic route of some plasma membrane proteins. TfR utilizes a direct route from Golgi to basolateral membrane that is established as the epithelial monolayer matures.

protein sorting | clathrin adaptors | endosomes | polarized secretion | epithelial cells

Epithelial cells segregate plasma membrane proteins into apical and basolateral domains, which is essential for their key role as selective barriers between the outside and the inside of an organism (1, 2). Over the past three decades, substantial progress has been made in characterizing intracellular routes followed by apical and basolateral proteins and the machinery involved in their polarized trafficking (2, 3). Apical sorting signals include glycosylphosphatidylinositol anchors (4, 5), specialized transmembrane domains (6–8), *N*- and *O*-glycans (9, 10), and cytoplasmic determinants (2, 11); these signals mediate apical sorting through interaction with lipid rafts, lectins, or cytoplasmic motors (2, 12). Basolateral sorting signals include tyrosine motifs e.g., in low-density lipoprotein receptor (LDLR) and vesicular stomatitis virus G (VSVG) protein (13, 14), dileucine and monoleucine motifs (15–17), and pleomorphic sequences, as in polymeric Ig receptor (pIg-R) (18), transferrin receptor (TfR) (19), and neural cell adhesion molecule (20); these signals mediate basolateral sorting by means of clathrin and nonclathrin adaptors (2). Classical studies have shown that apical and basolateral proteins are sorted in the biosynthetic route, in the trans-Golgi network (TGN) (21, 22). Additionally, recycling basolateral receptors such as LDLR or TfR are sorted every few minutes after internalization back to the cell surface in recycling endosomes. Sorting signals in the biosynthetic and recycling routes are believed to be structurally similar (23, 24) although detailed studies have shown that they are different in the case of TfR (19).

Ultimately, elucidation of the epithelial sorting mechanisms requires the identification of which protein or adaptor recognizes each sorting signal and the pathway and compartment that harbors the sorting event. To date, only two basolateral sorting adaptors have been identified, AP1 (25) and AP4 (26), but the pathway or compartment where they perform their sorting function remains controversial. Of these two, only AP1 has been studied in some detail. AP1 has two variants, AP1A and AP1B, which differ only in their medium, sorting-signal binding subunits, μ1A and μ1B; the latter is expressed predominantly in epithelial cells (25). The epithelial cell line LLC-PK1 lacks μ1B and missorts some basolateral markers, including TfR and LDLR (27–29). Early electron microscopy studies suggested that AP1B sorted basolateral proteins at a TGN subdomain devoid of conventional TGN markers (30). However, functional studies from our laboratory revealed that LLC-PK1 cells did not missort LDLR in the biosynthetic route but, rather, in the recycling route (29) (reviewed in refs. 2 and 31), in agreement with the predominant endosomal localization of transfected μ1B (29, 32). However, studies over the past decade have shown that some newly synthesized plasma membrane proteins move from TGN to recycling endosomes (33–38), suggesting that the latter could act as a common sorting site in both routes for at least some basolateral proteins (2, 12, 31).

To clarify this controversy, we evaluated the sorting role of AP1B in the established prototype epithelial cell line, Madin–Darby canine kidney (MDCK) (39), using a loss-of-function approach. We generated μ1B knocked-down MDCK cell lines and studied the trafficking routes of TfR and VSVG protein. A recent paper (40) reported AP1B silencing in MDCK cells but did not address its site of function. Our results demonstrate that AP1B functions in both the biosynthetic and recycling routes of MDCK cells, consistent with its localization in recycling endosomes, which are themselves part of the biosynthetic route. In the case of TfR, an AP1B-independent route develops as the

Author contributions: D.G. designed research; D.G., A.D., and E.P. performed research; D.G., C.O., A.S., R.S., and A.G. contributed new reagents/analytic tools; D.G. and E.R.-B. analyzed data; and D.G. and E.R.-B. wrote the paper.

The authors declare no conflict of interest.

Abbreviations: LDLR, low-density lipoprotein receptor; MDCK, Madin–Darby canine kidney; TfR, transferrin receptor; TGN, trans-Golgi network; VSVG, vesicular stomatitis virus G protein.

§To whom correspondence should be addressed. E-mail: boulan@med.cornell.edu.

This article contains supporting information online at www.pnas.org/cgi/content/full/0610700104/DC1.

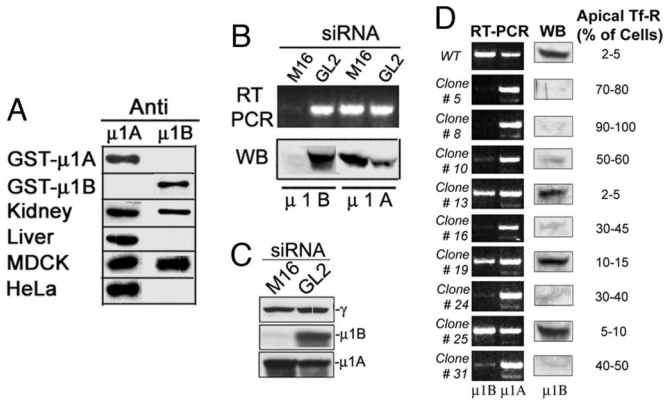

Fig. 1. Construction of permanently μ1B knockdown MDCK clones. (*A*) Rabbit antibodies were raised against μ1A and μ1B and tested by Western blot analysis against GST-tagged antigen and various tissue lysates (50 μg of protein). The anti-μ1B antibody showed no reactivity against rat (kidney, liver), human, or dog μ1A protein. (*B*) MDCK cells were transfected with μ1B-M16 or GL2-siRNA by electroporation and processed 72 h later for RT-PCR and Western blot. These cells are efficiently depleted of μ1B mRNA and protein. (*C*) MDCK cells were electroporated with m1B-M16 or GL2-siRNA three consecutive times at 3-d intervals and analyzed by Western blot. m1B-M16 siRNA results in undetectable levels of μ1B and increased levels of μ1A without altering γ-adaptin levels. (*D*) Puromycin-resistant clones were generated upon MDCK transfection with pSuper-μ1B-M16 vector. The extent of μ1B silencing was determined by RT-PCR and Western blot analysis. Two thirds of the screened clones displayed an effective depletion of μ1B. Each clone is infected with AdTfR for 30 h, and the fraction of cell displaying apical TfR is scored.

monolayer matures, suggesting that a different adaptor takes over transport from TGN to the basolateral membrane.

Results

Silencing μ1B with siRNA Promotes Apical Localization of TfR in Wild-Type MDCK Cells. RT-PCR analysis 72 h after transfection of siRNA sequences (41) selected from cloned canine μ1B revealed a potent silencing sequence (μ1B–M16) that caused ≈90% knockdown of μ1B protein and ≈1.5- to 2-fold increase in μ1A protein (Fig. 1 *A* and *B*) without altering the mRNA level of μ1A (Fig. 1*C*). This finding likely reflects a compensatory occupation by μ1A of AP1-adaptors left vacant by μ1B depletion. MDCK cells silenced with μ1B-M16 siRNA manifested neither noticeable morphological disruption of their epithelial organization (data not shown) nor a decreased transepithelial resistance (TER) (≈100–120 Ω·cm^2). A protocol of three sequential transfections with μ1B–M16 siRNA over a period of 9 d produced an effective depletion of μ1B protein with only a marginal effect on γ-adaptin expression (Fig. 1*C*). MDCK cells silenced with μ1B–M16 siRNA and infected for 36 h with either adenovirus-transducing human TfR (Ad-TfR) or human LDLR (Ad-LDLR), displayed a dramatic redistribution of TfR and LDLR to the apical membrane [supporting information (SI) Fig. 7], consistent with the observed LLC-PK1 phenotype (28, 29).

Generation of Stable μ1B Knockdown MDCK Cell Lines. To facilitate ulterior studies, we generated stable μ1B-knocked-down MDCK cell lines by transfecting the M16 sequence in a retroviral pSuper-vector (pSuper-μ1B-M16). Two types of clones were obtained (Fig. 1*D*). The majority (clones 5, 8, 10, 16, 24, and 31) showed strong depletion of μ1B and apical localization of TfR, transduced by an adenovirus vector (Fig. 1*D*). A small group (clones 13, 19, and 25) failed to silence μ1B and displayed μ1B protein and mRNA levels and basolateral TfR comparable to parental MDCK cells (Fig. 1*D*). Clone 8, μ1B-KD (>90% depletion of μ1B), and clone 25, control (μ1B level comparable

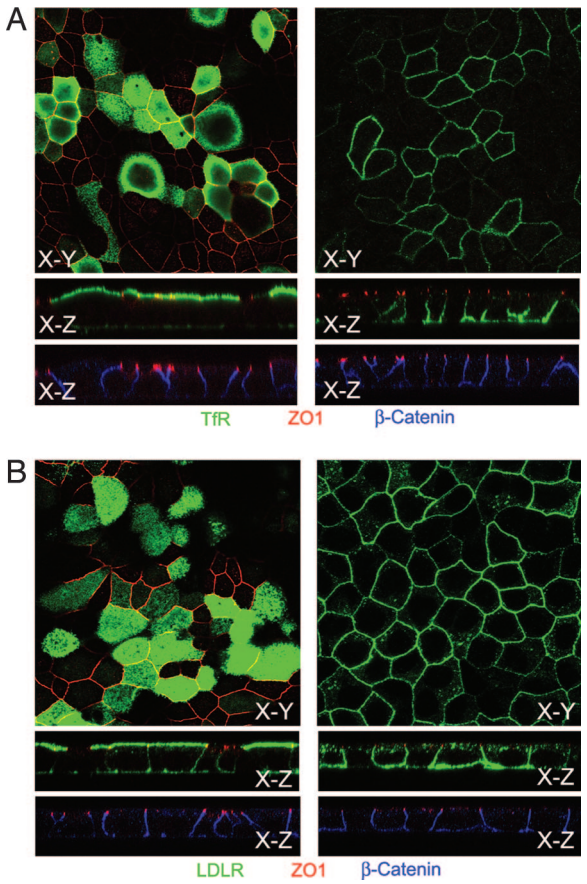

Fig. 2. μ1B-KD MDCK cells display apical TfR and LDLR. Control and μ1B-KD cells were infected with Ad-hTfR (*A*) or Ad-hLDLR (*B*) 3d after plating, fixed 36 h later, and processed for surface immunofluorescence with monoclonal antibodies against lumenal domains of TfR and LDLR, followed by brief permeabilization with Saponin 0.075% and immunostaining of β-catenin and ZO-1. (*Top*) XY sections at the apical membrane (μ1B-KD, *Left*) or at midcell (Control, *Right*). (*Middle* and *Bottom*) XZ sections.

to parental cells), were chosen for subsequent trafficking studies. Control and μ1B-KD cells quickly (≈24 h) built up epithelial monolayers with comparable tightness TER >80 Ω·cm^2 as more mature (3–6 d) monolayers: 94 ± 8 Ω·cm^2 (control), 91 ± 11 Ω·cm^2 (μ1B-KD), and 120 ± 16 Ω·cm^2 (parental). Parental cells displayed a TER spike of 365 Ω·cm^2 at 24 h that has been attributed to a developmental change in the ionic permselectivity of tight junctions (39). This spike was not observed in control or μ1B-KD cells (SI Fig. 8).

μ1B-KD MDCK Cells Displays Loss of Polarity of Transfected and Endogenous Basolateral Proteins. μ1B-KD MDCK cells, confluent for 4.5 d, displayed a dramatic apical redistribution of transfected TfR (Fig. 2*A*) and LDLR (Fig. 2*B*) that contrasted with the basolateral localization of these proteins in control and parental MDCK cells (Fig. 2 *A* and *B* and data not shown). Moreover, domain-selective biotinylation, followed by Western blot analysis of polarized (4.5 d) μ1B-KD MDCK cells revealed a dramatic redistribution of TfR and β1-integrin (≈40%) to the apical surface, whereas other basolateral proteins were either marginally affected (e.g., E-cadherin) or not affected (e.g., the β-subunit of Na, K-ATPase). Two apical markers, gp114 (42) and gp135 (43), displayed normal polarity in μ1B-KD MDCK cells (Fig. 3).

A Surface Capture Assay to Measure Polarized Biosynthetic Delivery and Recycling of TfR. Existing biotin-based assays do not allow a precise measurement of the polarized delivery of highly

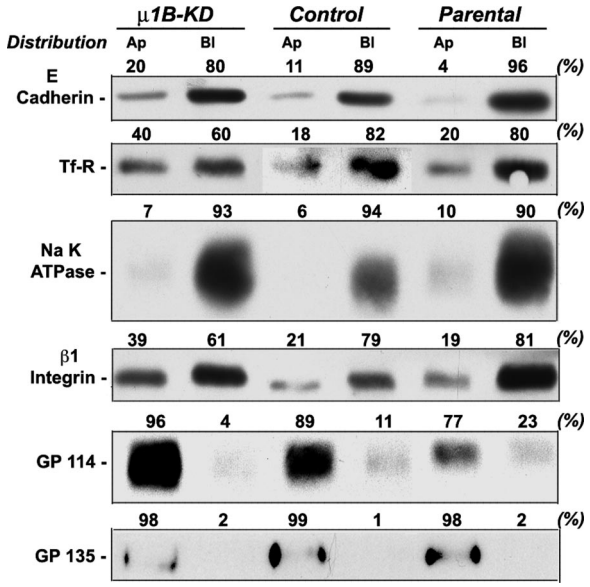

Fig. 3. Decreased polarity of endogenous basolateral markers in μ1B-KD MDCK. The steady-state surface distribution of some basolateral and apical membrane proteins in fully polarized (4.5-d) parental, control, and μ1B-KD MDCK cells was determined by using Western blot analysis after domain-selective biotinylation.

endocytic receptors, such as TfR (44, 45). To overcome this limitation, we developed a new surface delivery assay that captures [^{35}S]-pulsed TfR with biotin-Tf (B-Tf) added to the apical or basolateral media of MDCK cells grown on filters (Fig. 4*A*). A key step of this method is to lyse cells at pH 5.5 to preserve the integrity of B-Tf/TfR complex in the endosomal system, which is later retrieved with Avidin-Sepharose. According to whether B-Tf is added immediately after a [^{35}S]-pulse (Fig. 4*A Left*) or 3.5 h after the pulse (Fig. 4*A Right*), the assay measures biosynthetic delivery or recycling of TfR.

μ1B Silencing Disrupts Recycling but Not Biosynthetic Delivery of TfR in 4.5-d Confluent MDCK. Parental, control, and μ1B-KD MDCK cells infected with Ad-TfR were subjected to the biosynthetic delivery assay (Fig. 4*A Left*). Newly synthesized TfR reached the cell surface with similar kinetics in parental, control, and μ1B-KD cells ($T_{1/2} \approx$ 33, 38, and 38 min, respectively) (Fig. 4*B*). Delivery in all cases was predominantly basolateral, with a slightly larger fraction missorted to the apical surface in μ1B-KD cells (23.8 ± 5.1%) versus (12.5 ± 7.8%) in parental and (14.4 ± 4.7%) in control cells after 70 min of chase (Fig. 4*B* and SI Table 1).

In contrast, the recycling assay (Fig. 4*A Right*) showed that μ1B-KD MDCK cells recycled apically a major fraction of TfR, ≈48.8 ± 18.2% (n = 5), compared with parental and control MDCK cells, which recycled most of TfR basolaterally (84.9 ± 7.3% and 81.2 ± 5.3%, respectively) within 30 min (Fig. 4*C*). This major disruption of TfR recycling was also observed by using a variation of the recycling assay that measured the washout of internalized B-Tf (Fig. 4*D*). Overall, these experiments demonstrate that in 4.5-d confluent MDCK cells: (*i*) AP1B sorts TfR in the recycling route, consistent with the demonstrated function of this adaptor in LLC-PK1 cells (29) and (*ii*) biosynthetic delivery of TfR is largely AP1B-independent.

AP1B Functions in the Biosynthetic Route of TfR in Recently Polarized MDCK Cells. Studies in MDCK cells (39, 46–48) and in FRT cells (49, 50) have shown that polarity develops in stages over several days and that this correlates with changes in polarized trafficking routes. Hence, we decided to investigate whether the biosynthetic route of TfR might use AP1B during early stages of polarization of the monolayer. Analysis of biosynthetic delivery of TfR with our capture assay (Fig. 4*A Left*) in 1- to 1.5-d confluent MDCK cells infected with Ad-TfR by two slightly different protocols, revealed a striking difference with our observations in 4.5-d confluent MDCK cells. Whereas parental and control MDCK cells delivered 70–90% of newly synthesized TfR to the basolateral surface, μ1B-KD cells missorted ≈50% of TfR to the apical surface (Fig. 4 *E* and *F*). Additional experiments performed after 2 d of confluency revealed a similar AP1B dependence, although with decreasing intensity as the monolayer matured (data not shown). Control experiments showed that this result cannot be attributed to increased transduction of TfR or deficient tight junctions in early confluent MDCK cells (SI Fig. 9). Rather, the experiments are consistent with the development of an AP1B-independent biosynthetic route for TfR as MDCK monolayers mature.

AP1B Functions in the Biosynthetic Route of VSVG Protein. VSVG protein, a basolateral marker in MDCK cells (51), is delivered vectorially to the basolateral surface of MDCK cells (52). Using a modified version of our original biotin targeting assay (44), we studied the biosynthetic delivery of this protein in parental and μ1B-KD MDCK cells after infection with Ad-VSVG for 24 h. Strikingly, whereas parental MDCK cells delivered VSVG exclusively to the basolateral membrane, μ1B-KD cells missorted a large proportion of VSVG to the apical surface (Fig. 5). Comparable results were observed by immunofluorescence analysis of cells infected with an adenovirus transducing a VSVG-GFP chimera (53) for 24 h at 39°C, followed by 2 h incubation at 32°C (SI Fig. 10). These experiments demonstrate that a substantial fraction of VSVG utilizes an AP1B-dependent route to the basolateral surface in fully polarized MDCK cells.

μ1B Localizes to Endosomal Fractions in 0- and 4-d Confluent MDCK Cells. Immunofluorescence experiments with LLC-PK1 cells functionally reconstituted with μ1B show better colocalization of μ1B with Tf-labeled endosomes than with Golgi markers (29, 32). Cell fractionation studies in MDCK cells revealed a similar pattern for endogenous μ1B, i.e., a preferential sedimentation with TfR-rich fractions rather than with Golgi fractions; this was also the case for MDCK cells just reaching confluency (C-0 d) or confluent for 4 d (C-4 d) (Fig. 6 and SI Fig. 11). These data support the concept that AP1B carries out its basolateral sorting function in the endosomal compartment.

Discussion

Unlike regular biotin targeting assays, which quantify only the receptor pool at a given time at the cell surface, our TfR surface capture assay quantifies, depending on the experimental design, the total receptor pool delivered to the cell surface during biosynthesis or during recycling. Utilization of this assay in μ1B-depleted MDCK cells confluent for 4.5 d (104 h: 72 h of plating plus 32-h infection with adenoviruses) demonstrated only a slight alteration in the biosynthetic delivery of TfR to the basolateral membrane; by contrast, recycling of TfR was deeply disrupted, with approximately half of the receptor diverted to the apical membrane (Fig. 4). These experiments demonstrate that, in MDCK cells polarized for ≈4.5 d, AP1B exerts its sorting role on TfR only in the recycling route and not in the biosynthetic route, in agreement with our previous functional observations with LDLR in polarized LLC-PK1 monolayers (29). In contrast, the biosynthetic route of VSVG protein was disrupted to a large extent in μ1B-KD MDCK cells polarized for 4.5 d. Thus, 4.5-d confluent MDCK cells appear to have μ1B-dependent and μ1B-independent routes to the basolateral membrane. Whereas the YXXΦ basolateral sorting motif of VSVG protein may be

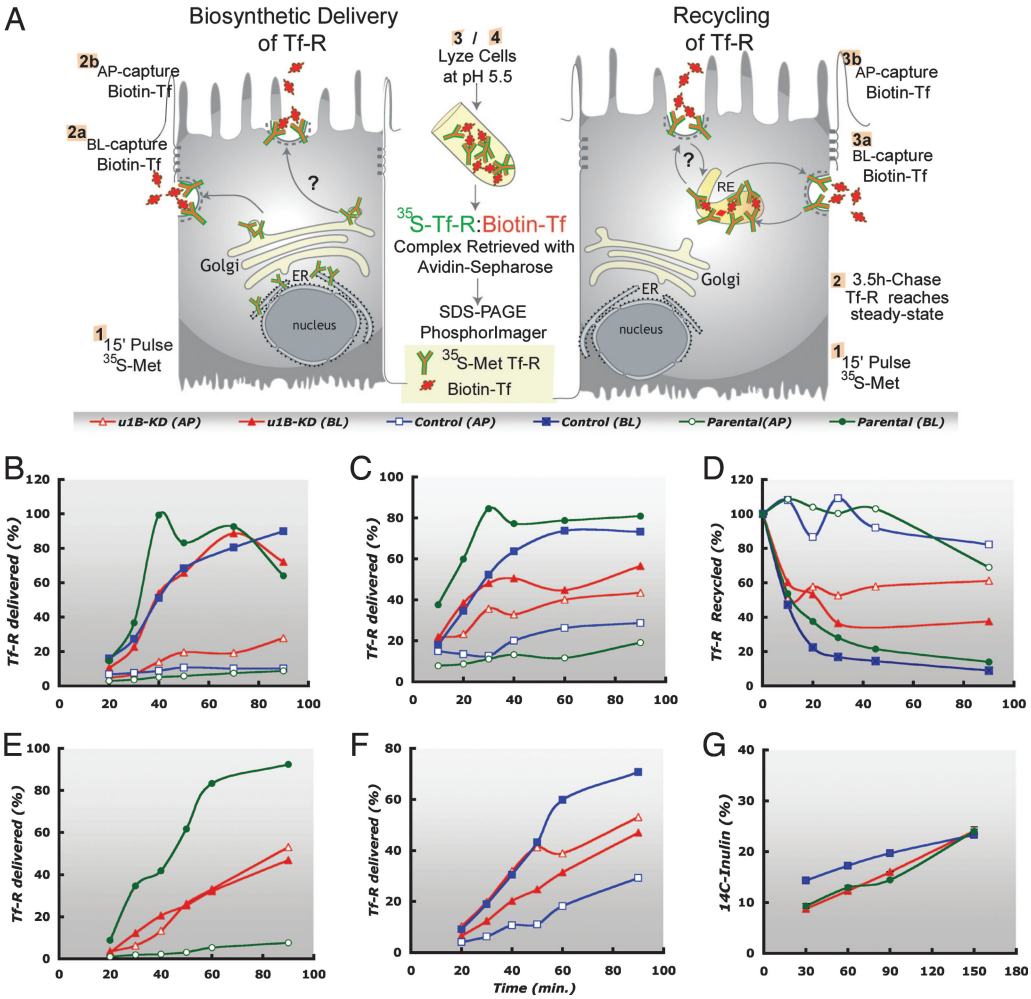

Fig. 4. Biosynthetic delivery and recycling of TfR in control and μ1B-KD MDCK. (*A*) Assays to quantify biosynthetic delivery or recycling of TfR. MDCK cells infected with AdTfR are pulsed with [^{35}S]Met/Cys for 13 min. For biosynthetic delivery (*Left*), cells are immediately chased with excess unlabeled met/cys in the presence of Biotin-Tf (B-Tf) added to apical or basal side. For recycling (*Right*) a 3.5-h chase follows the pulse before incubation with B-Tf. Cells are lysed at pH 5.5, and the B-Tf/TfR complex was retrieved with Avidin-Sepharose. (*B*) Biosynthetic sorting of TfR in 4.5-d confluent MDCK cells. Control and parental MDCK cells targeted 12–15% of newly synthesized TfR to the apical surface. μ1B-KD MDCK cells targeted ≈23% of newly synthesized TfR to the apical surface (see text and SI Table 1). (*C*) Recycling of TfR. Whereas control and parental MDCK cells recycled >80% of TfR to the basolateral membrane, μ1B-KD cells recycled more than ≈50% of TfR to the apical membrane (see SI Table 1). (*D*) Modified version of recycling assay. Biotin-Tf was added to both apical and basal media during the last 90 min of the 3.5-h chase. Subsequently, cells were exposed to an excess of Tf added to either apical or basolateral side. In parental and control cells, B-Tf is displaced by Tf efficiently only when added basolaterally, whereas in μ1B-KD MDCK cells, >45% of B-Tf was displaced by Apical Tf. (*E*) Biosynthetic delivery of TfR in 1- to 1.5-d confluent MDCK cells. Confluent parental, control, and μ1B-KD MDCK cells were infected with Ad-TfR, trypsinized 6 h later, plated at confluency on polycarbonate filters, and used to measure biosynthetic delivery of TfR 24 h later, as in *A Left*. (*F*) Alternatively, cells after 8 h of plating were infected with Ad-hTfR for 24 h and then assayed for biosynthetic delivery of TfR. Note the nonpolarized delivery of TfR by μ1B-KD MDCK in *E* and *F*. (*G*) Monolayers formed by μ1B-KD, control and parental MDCK cells under conditions similar to those used in *E* and *F* display similar low permeability to [^{3}H]inulin.

responsible for its AP1B dependence (14), it is likely that the nonconventional basolateral signal of TfR (19) might account for its AP1B-independent route to the basolateral membrane.

Various reports that go back a decade have described a transendosomal route for several newly synthesized plasma membrane proteins, e.g., TfR itself (33), asialoglycoprotein receptor (37), polymeric Ig receptor (54), E-cadherin (36), and, more recently, VSVG protein (38) (reviewed in ref. 12). If the biosynthetic route of basolateral proteins indeed intersected the recycling route of MDCK cells, which our functional studies indicate is the major functional locus of AP1B, we would expect that μ1B-KD MDCK cells would missort newly synthesized plasma membrane proteins. In our initial studies with MDCK cells polarized for 4.5 d, we observed this scenario for VSVG but not for TfR. However, it is well documented that MDCK monolayers plated at confluency develop their tight junctions within ≈12 h (39) and progressively refine their cytoplasmic and surface polarity, as well as their tight junction permeability, with additional days in culture (39, 46–48). Because we noticed that practically all studies on the transendosomal biosynthetic route had been carried out in either fibroblastic cell lines (37) or in nonpolarized or recently polarized MDCK cells (33, 36, 38), we decided to study the targeting of TfR in MDCK cells at different days after confluency. Strikingly, recently polarized (1- to 1.5-d) monolayers of μ1B-KD MDCK cells (but not parental or control cells) missorted TfR apically in the biosynthetic route but developed an efficient basolateral route with additional days in culture. Our results are consistent with the following model: as MDCK cells refine their polarity, they develop a direct route from the Golgi complex to the basolateral membrane that bypasses recycling endosomes. Basolateral adaptors, e.g., AP4 (26) or other candidate adaptors, e.g., AP3 (55) or AP1A might become activated or might compensate for the knockdown of AP1B as MDCK

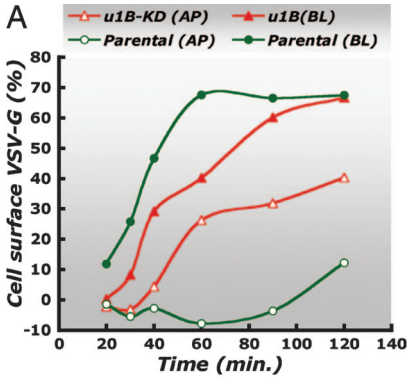

B

	AVERAGE ± STDEV
μ1B-KD	0.650±0.046
Parental	0.120±0.058

Fig. 5. Biosynthetic delivery of VSVG protein is disrupted in fully polarized (4.5 d) confluent μ1B-KD MDCK cells. (*A*) Parental and μ1B-KD MDCK cells were infected for 24 h with Ad-VSVG, pulsed with [^{35}S]Met/Cys, chased for the times indicated, and biotinylated from the apical or basolateral sides. VSVG from each sample was immunoprecipitated and processed for a biotin-targeting assay (45). Value represents the percent at apical or basolateral surfaces of total VSVG. Note the polarized basolateral delivery of VSVG in parental MDCK cells and the depolarized delivery of VSVG in μ1B-KD MDCK cells. (*B*) Shows the average ± standard deviation values of the apical/basolateral delivery ratio after a 2-h chase at 32°C for μ1B-KD and parental MDCK cells.

cells refine their polarity. An alternative possibility, i.e., that AP1B might change its functional site from the Golgi complex to recycling endosomes as MDCK cells polarize cannot be fully discarded at this time. Although immunofluorescence studies of subconfluent LLC-PK1 show preferential expression of AP1B in endosomes rather than in TGN (29, 32), and our cell fractionation studies detect preferential association of μ1B with TfR-rich endosomal membranes at early- and late-confluency stages, our data cannot eliminate the possibility that a small very dynamic pool of AP1B plays a sorting role in the TGN. However, function blocking antibodies against μ1B block biosynthetic trafficking of VSVG protein in an

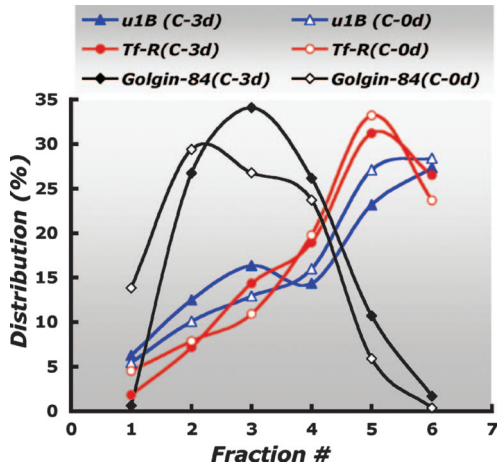

Fig. 6. Sedimentation analysis of AP1B distribution. MDCK cells, confluent for 0 (C-0 d) or 4 d (C-4 d) were homogenized and analyzed by sucrose density centrifugation, as described in *Materials and Methods.* Gradient fractions were analyzed by SDS/PAGE and Western blot analysis (original gels in SI Fig. 11). The values represent the percent of the various markers in a given fraction. Note that μ1B sediments preferentially in higher-density fractions that contain TfR.

endosomal compartment rather than in the TGN (J. Cancino, A.S., C.O., I. Yuseff, D.G., G. Mardones, P. Henklein, E.R.-B., and A.G., unpublished work) supporting a scenario in which AP1B functions in recycling endosomes.

We speculate that centralization of all biosynthetic and recycling plasma membrane protein sorting into endosomes might be advantageous for nonpolarized, motile cells, because it would facilitate quick changes in direction of membrane flow in both biosynthetic and recycling routes in response to external cues. On the other hand, the segregation of sorting roles between biosynthetic and recycling routes after polarization may allow for more precise sorting of plasma membrane receptors and transporters, necessary to perform the vectorial functions characteristic of the epithelium. These interesting hypotheses certainly deserve additional study.

Materials and Methods

Antibodies to μ1A and μ1B. Antibodies to μ1A and μ1B were elicited in rabbits by injecting CKVLFDNTGRGKS (μ1A) or CRVLFELTGRSKN (μ1B) peptides coupled to mollusk *concholepas-concholepas* hemocyanin (Blue Carrier; Biosonda Biotechnology, Santiago, Chile). Specific antibodies were retrieved by antigen-affinity purification with GST-μ1B or GST-μ1A. Antibodies were tested by Western blot against GST-tagged proteins and lysates obtained from various sources (SI Fig. 7).

siRNA Knockdown and Permanent Silencing of μ1B in MDCK Cells. An available algorithm (siRNA at Whitehead, http://jura.wi.mit-.edu/bioc/siRNAext/home.php) was used to identify candidate sequences for siRNA silencing in canine μ1B. The chosen μ1B-targeted siRNA (μ1B-M16) AACAAGCTGGTGACTG-GCAAA and a control luciferase siRNA (GL2-siRNA) were custom synthesized (Dharmacon, Lafayette, CO). To transfect siRNA, trypsinized MDCK cells were resuspended in Nucleofector solution (Amaxa, Gaithersburg, MD) at 4×10^6 cells per 100 μl, added to 160 pmol of siRNA oligonucleotide, and electroporated as recommended by the manufacturer.

To generate stable knockdown clones of μ1B, a pair of custom-synthesized sense (5′-GATCCCCCAAGCTGGTGACTG-GCAAATTCAAGAGATTTGCCAGTCACCAGCTTGTT-TTTA-3′) and antisense (5′-AGCTTAAAAACAAGCTG-GTGACTGGCAAATCTCTTGAATTTGCCAGTCACCA-GCTTGGGG-3′) 60-mer oligonucleotides encoding the 19-mer μ1B-targeted sequence (μ1B-M16) and convenient BglII and HindIII restriction sites were annealed and cloned into a pSuper.retro.puro vector (Oligoengine Seattle, WA) following manufacturer's instructions. The resulting vector, pSuper-μ1B-M16, was transfected into MDCK cells by electroporation (Amaxa). Puromycin-resistant clones were picked and further characterized by RT-PCR, Western blot analysis, and surface immunofluorescence.

Assay for Biosynthetic Delivery and Recycling of TfR. Confluent MDCK cells (72 h or as otherwise indicated) were infected with Ad-TfR for 28–36 h, pulse-labeled for 13 min with 0.5 mCi/ml (1 Ci = 37 GBq) of [^{35}S]Met/Cys ([^{35}S]-Express) and immediately chased at 37°C in serum-free DMEM (SF-DMEM) supplemented with BSA 0.75% and 50 μg/ml biotinylated Tf (B-Tf) added to the apical or basolateral side. After washing excess B-Tf with ice-cold HBSS supplemented with 0.5% BSA, cells were lysed for 30 min at 4°C with lysis buffer (LB/5.5) containing 40 mM sodium acetate (pH 5.5), 150 mM NaCl, 30 mM KCl, 2.5 mM EDTA, 1.5%, Triton X-100, 1% albumin, and a mixture of protease inhibitor (CPI) containing 1 mM PMSF, 15 μg/ml leupeptin/ pepstatin/antipain and 75 μg/ml benzamidine-ClH. The B-Tf/TfR complex was then retrieved with Avidin-Sepharose. Samples were processed by electrophoresis on SDS-gel and analyzed by PhosphorImager (Molecular Dynamics, Sunnyvale, CA). For TfR recycling assays, cells were processed exactly as described above, except that, after [^{35}S]-pulse, the cells were chased for a total of 3.5 h (2 h with complete and 1.5 h

with SF-DMEM) to allow [^{35}S]-labeled TfR to equilibrate within the endosomal compartment. For additional information, see *SI Materials and Methods.*

We thank Dr. Alicia Solorzano for helpful advice with molecular biology procedures, David Cohen and Anne Musch for advice with manipulation of adenoviruses, Aparna Lakkaraju for skillful help with schemes in Fig. 4, and Fernando Diaz for additional data confirming our VSVG results. This work was supported by National Institutes of Health Grants GM 34107 and EY08538 (to E.R.-B.), the Dyson Foundation, the Research to Prevent Blindness Foundation, El Fondo de Centros de Excelencia en Investigación Grant 13980001 (to A.G.), Millennium Institute for Fundamental and Applied Biology, and the Ministerio de Planificación y Cooperación de Chile.

1. Cereijido M, Contreras RG, Shoshani L (2004) *Physiol Rev* 84:1229–1262.
2. Rodriguez-Boulan E, Kreitzer G, Musch A (2005) *Nat Rev Mol Cell Biol* 6:233–247.
3. Mostov K, Su T, ter Beest M (2003) *Nat Cell Biol* 5:287–293.
4. Brown DA, Crise B, Rose JK (1989) *Science* 245:1499–1501.
5. Lisanti M, Caras IP, Davitz MA, Rodriguez-Boulan E (1989) *J Cell Biol* 109:2145–2156.
6. Skibbens JE, Roth MG, Matlin KS (1989) *J Cell Biol* 108:821–832.
7. Kundu A, Avalos RT, Sanderson CM, Nayak DP (1996) *J Virol* 70:6508–6515.
8. Scheiffele P, Roth MG, Simons K (1997) *EMBO J* 16:5501–5508.
9. Fiedler K, Simons K (1995) *Cell* 81:309–312.
10. Yeaman C, Le Gall AH, Baldwin AN, Monlauzeur L, Le Bivic A, Rodriguez-Boulan E (1997) *J Cell Biol* 139:929–940.
11. Tai AW, Chuang JZ, Bode C, Wolfrum U, Sung CH (1999) *Cell* 97:877–887.
12. Ellis MA, Potter BA, Cresawn KO, Weisz OA (2006) *Am J Physiol* 291:F707–F713.
13. Matter K, Hunziker W, Mellman I (1992) *Cell* 71:741–753.
14. Thomas DC, Roth MG (1994) *J Biol Chem* 269:15732–15739.
15. Hunziker W, Fumey C (1994) *EMBO J* 13:2963–2969.
16. Wehrle-Haller B, Imhof BA (2001) *J Biol Chem* 276:12667–12674.
17. Deora AA, Gravotta D, Kreitzer G, Hu J, Bok D, Rodriguez-Boulan E (2004) *Mol Biol Cell* 15:4148–4165.
18. Casanova JE, Apodaca G, Mostov KE (1991) *Cell* 66:65–75.
19. Odorizzi G, Trowbridge IS (1997) *J Cell Biol* 137:1255–1264.
20. Le Gall AH, Powell SK, Yeaman CA, Rodriguez-Boulan E (1997) *J Biol Chem* 272:4559–4567.
21. Rindler MJ, Ivanov IE, Plesken H, Rodriguez-Boulan E, Sabatini DD (1984) *J Cell Biol* 98:1304–1319.
22. Fuller SD, Bravo R, Simons K (1985) *EMBO J* 4:297–307.
23. Aroeti B, Mostov KE (1994) *EMBO J* 13:2297–2304.
24. Matter K, Whitney JA, Yamamoto EM, Mellman I (1993) *Cell* 74:1053–1064.
25. Ohno H, Tomemori T, Nakatsu F, Okazaki Y, Aguilar RC, Foelsch H, Mellman I, Saito T, Shirasawa T, Bonifacino JS (1999) *FEBS Lett* 449:215–220.
26. Simmen T, Honing S, Icking A, Tikkanen R, Hunziker W (2002) *Nat Cell Biol* 4:154–159.
27. Roush DL, Gottardi CJ, Naim HY, Roth MG, Caplan MJ (1998) *J Biol Chem* 273:26862–26869.
28. Folsch H, Ohno H, Bonifacino JS, Mellman I (1999) *Cell* 99:189–198.
29. Gan Y, McGraw TE, Rodriguez-Boulan E (2002) *Nat Cell Biol* 4:605–609.
30. Folsch H, Pypaert M, Schu P, Mellman I (2001) *J Cell Biol* 152:595–606.
31. Folsch H (2005) *Trends Cell Biol* 15:222–228.
32. Folsch H, Pypaert M, Maday S, Pelletier L, Mellman I (2003) *J Cell Biol* 163:351–362.
33. Futter CE, Connolly CN, Cutler DF, Hopkins CR (1995) *J Biol Chem* 270:10999–11003.
34. Apodaca G, Katz LA, Mostov KE (1994) *J Cell Biol* 125:67–86.
35. Orzech E, Cohen S, Weiss A, Aroeti B (2000) *J Biol Chem* 275:15207–15219.
36. Lock JG, Stow JL (2005) *Mol Biol Cell* 16:1744–1755.
37. Laird V, Spiess M (2000) *Exp Cell Res* 260:340–345.
38. Ang AL, Taguchi T, Francis S, Folsch H, Murrells LJ, Pypaert M, Warren G, Mellman I (2004) *J Cell Biol* 167:531–543.
39. Cereijido M, Robbins ES, Dolan WJ, Rotunno CA, Sabatini DD (1978) *J Cell Biol* 77:853–880.
40. Anderson E, Maday S, Sfakianos J, Hull M, Winckler B, Sheff D, Folsch H, Mellman I (2005) *J Cell Biol* 170:595–605.
41. Reynolds A, Leake D, Boese Q, Scaringe S, Marshall WS, Khvorova A (2004) *Nat Biotechnol* 22:326–330.
42. Fullekrug J, Shevchenko A, Shevchenko A, Simons K (2006) *BMC Biochem* 7:8.
43. Herzlinger DA, Ojakian GK (1984) *J Cell Biol* 98:1777–1787.
44. Le Bivic A, Real FX, Rodriguez-Boulan E (1989) *Proc Natl Acad Sci USA* 86:9313–9317.
45. Sargiacomo M, Lisanti M, Graeve L, Le Bivic A, Rodriguez-Boulan E (1989) *J Memb Biol* 107:277–286.
46. Balcarova-Stander J, Pfeiffer SE, Fuller SD, Simons K (1984) *EMBO J* 3:2687–2694.
47. Nelson WJ, Veshnock PJ (1986) *J Cell Biol* 103:1751–1765.
48. Vega Salas DE, Salas PJ, Gundersen D, Rodriguez-Boulan E (1987) *J Cell Biol* 104:905–916.
49. Zurzolo C, Le Bivic A, Quaroni A, Nitsch L, Rodriguez-Boulan E (1992) *EMBO J* 11:2337–2344.
50. Marzolo MP, Bull P, Gonzalez A (1997) *Proc Natl Acad Sci* 94:1834–1839.
51. Rodriguez-Boulan E, Pendergast M (1980) *Cell* 20:45–54.
52. Pfeiffer S, Fuller SD, Simons K (1985) *J Cell Biol* 101:470–476.
53. Keller P, Toomre D, Diaz E, White J, Simons K (2001) *Nat Cell Biol* 3:140–149.
54. Orzech E, Cohen S, Weiss A, Aroeti B (2000) *J Biol Chem* 275:15207–15219.
55. Nishimura N, Plutner H, Hahn K, Balch WE (2002) *Proc Natl Acad Sci USA* 99:6755–6760.